Mapping Rice Paddy Areas in Nueva Ecija Using Temporal Sentinel -1 SAR Imagery

Jann Rovic Cueto[1], Jessah Mei Allard[2], Johanne Mae Obras[1], Allysa Maxine De Asis[1], Arnel Galut[1], Roland Dayrit[3], John Allen Tandoc[3], Mark Angelo Purio[3, 4]

[1]Dept. of Earth and Space Science, Rizal Technological University, Boni, Mandaluyong, Philippines - (abm11c.cueto.jannrovic, obrasjohanne, allysamaxined, arnelgalut15)@gmail.com
[2]Dept. of Geology, Caraga State University, Butuan, Philippines - jessahmei.allard@carsu.edu.ph
[3]Dept. of Electronics Engineering, Adamson University, Manila, Philippines - (roland.dayrit, john.allen.tandoc)@adamson.edu.ph
[4]Space Technologies and Applications Research Laboratory, Adamson University, Manila, Philippines - markangelo.purio@adamson.edu.ph

Keywords: Rice crops, Classification, Agricultural land, Crop monitoring, Landcover.

Abstract

Remote Sensing is proven to be helpful in various ways, and for an agricultural country like the Philippines, mapping in farmlands is not that common. Using the Sentinel 1 Synthetic Aperture Radar (SAR) data, the study reveals rice paddy classification brought by supervised machine learning on the municipality of Guimba, in Nueva Ecija - the Rice Bowl Capital of the country. The study in Guimba, Nueva Ecija, addresses the absence of comprehensive rice classification studies, focusing on creating a classified rice paddy map and assessing spectral indices (NDMI, NDVI, NDWI) using synthetic aperture radar and optical imager. Results show successful differentiation between rice and non-rice paddies. Temporal analysis emphasizes monitoring water availability, soil moisture, and vegetation health. Despite signs of overprediction in the CART model, its effectiveness in mapping rice paddies is notable. The spatial distribution maps contribute to targeted monitoring, enabling efficient interventions and improved agricultural practices. This research highlights the inherent use of remote sensing in rice crop management, offering valuable insights for farmers and country's food security.

1. Introduction

1.1 Background of the Study

About 90% of the world’s rice is produced in Asia, according to (Gutaker et al., 2020). As it is a staple crop in many regions, some countries produce rice for their supply and consumption, such as the Philippines. Out of 30 million hectares of agricultural land, about 4.81 million hectares are specified for rice production (Silva et al., 2017)**.** In 2020, rice production in the Philippines reached 19.44 million metric tons, where the biggest contributions were the regions of Central Luzon, Cagayan Valley, and Ilocos (Agoot, 2020). The country’s biggest rice producer is Region 3, Central Luzon. Due to its capability to produce millions of metric tons of rice, it is known as the Rice Capital of the Philippines and comprises seven provinces namely Aurora, Nueva Ecija, Bulacan, Pampanga, Tarlac, Bataan, and Zambales. Rice is cultivated in the Philippines primarily during the wet season, from June to early October mostly in naturally irrigated areas. Cultivation continues during the dry, to hot-dry season (late October to May) for areas with specific irrigation facilities (Raviz et al., 2016)**.** The researchers will specifically classify the rice paddies located in Guimba, a district in Nueva Ecija. To classify the rice paddies in this district, the researchers utilized the Sentinel 1 - Synthetic Aperture Radar (SAR) and Sentinel 2 - Multispectral Satellite Imagery (MSI) and accessed its open-sourced data from Google Earth Engine (GEE) geospatial platform from June to October 2021. In relation to this, the Municipality of Guimba was specifically decided for this study due to having the lowest cloud cover observed, therefore allowing the study to have an increased precision in the mapping process. This study aims to provide a specific and precise rice paddy mapping in the Nueva Ecija and Municipality of Guimba from remote sensing satellite images through a machine learning approach involving the following: (1) Random Forest Trees, (2) Classification and Regression Trees (CART), and (3) Gradient Tree Booster. Significantly, the researchers aim for the study to aid farmers in decision-making regarding water and moisture management, aiming to maximize harvests and minimize risks.

1.2 Objectives of the Study

1. Create a precise rice paddy map using supervised classification and utilize the use of cloud open-source platform for ease replication.

2. Monitor and assess the change of rice paddy indices in municipality of Guimba on wet season planting.

2. Materials and Methods

2.1 The Study Area

The study area of the rice mapping is Nueva Ecija Province, Philippines, located in the Central Luzon plains with an area of approximately 5,751.33 km² (Figure 1). The province experiences a humid subtropical climate, with mountainous terrain in the east, low hills in the north, and mainly plains in the central region. According to Global Forest Watch (2022), cropland is the main land use type in the study area, accounting for approximately 7.8%. And paddy rice is the main crop, accounting for 0.26%. A simple criterion was created upon choosing the district best for the rice paddy mapping. After gathering data from Sentinel 1 and Sentinel 2 Copernicus data catalogue through an open-access platform, the researchers set its data collection period from June to October 2021.Within the data gathered, Guimba had the lowest observed cloud cover. Furthermore, in this chosen study area, 40 hectares is considered as croplands (primarily used for farming), where about 18 hectares is known to be the rice paddies. Specifically, the researchers utilized remote sensing data, specifically the polarization and create a temporal logic color composite bands from Sentinel 1 data. From June to October 2021, there were a total of 12 images acquired. These underwent geometric

This contribution has been peer-reviewed. The double-blind peer-review was conducted on the basis of the full paper.
https://doi.org/10.5194/isprs-annals-X-5-2024-41-2024 | © Author(s) 2024. CC BY 4.0 License.

correction before applying the temporal logic color composite, which involved the vertical/horizontal polarization of the interferometric wide swath, providing 66 total annotated samples. This number accounts for 49 rice paddies and 17 non-rice paddies.

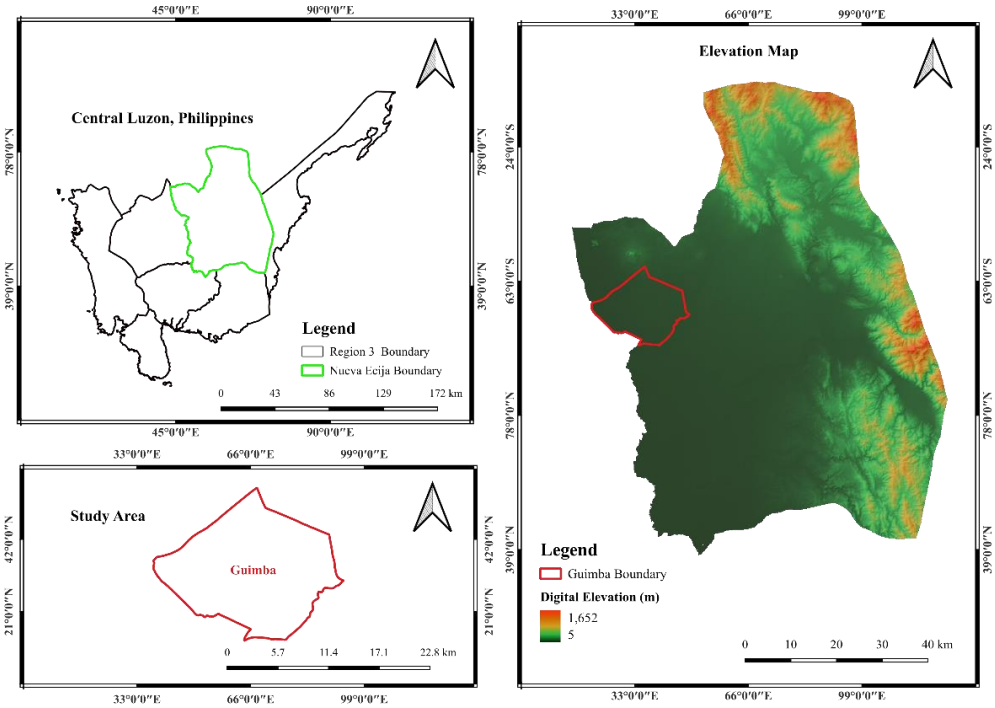

Figure 1. Study area.

No.	Date	No.	Date
1	08 June 2021	7	07 August 2021
2	20 June 2021	8	12 September 2021
3	02 July 2021	9	24 September 2021
4	14 July 2021	10	06 October 2021
5	20 July 2021	11	18 October 2021
6	26 July 26	12	30 October 2021

Table 1. The acquisition dates of Sentinel-1 images.

2.2 Supervised Classifications Models

This section presents the different model approach for the rice classification using supervised machine learning in Sentinel -1 SAR temporal images that are captured during the wet season planting window in Nueva Ecija.

2.2.1 Random Forest Trees

The random forest classifier employed in this study consisted of an ensemble of tree classifiers. Each classifier was constructed by sampling a random vector independently from the input vector (Breiman, 2001). The decision-making process involved each tree casting a unit vote for the most prevalent class to classify an input vector, as outlined by (Gislason et al., 2006). In this study, we used the random forest classifier which utilized a method of growing trees with randomly selected features at each node. To ensure consistency and reproducibility, hyperparameters were set. Specifically, the number of decision trees was set to 100, and a random seed of 42 was applied.

2.2.2 Classification and Regression Trees

Classification and regression trees (CART) are powerful machine learning methods that build predictive models by dividing data into smaller subgroups and fitting simple models within each. The flexibility of CART has drawn considerable attention in remote-sensing radar image classification. A hierarchical copula-based method for multisensory and multiresolution images, demonstrate a robustness against noise and speckle (Voisin et al., 2014). Using a decision tree based on remote sensing images, even outperformed the traditional maximum likelihood classification method in terms of accuracy (Qi et al., 2011).

2.2.3 Gradient Tree Booster

Gradient Tree Boosting, a powerful ensemble learning algorithm, leverages complex base learners like piecewise linear regression trees to build robust models (Shi et al., 2018). Its effectiveness extends beyond binary classification, tackling multi-label and multi-output regression through novel random output projections (Joly et al., 2019). This versatility makes it particularly well-suited for analyzing radar satellite images. For instance, a research study demonstrated its effectiveness in crop classification using PolSAR imagery, where tree and DART boosters significantly outperformed the simpler linear booster (Ustuner et al., 2019).

2.3 Land Cover and Land Use

The study utilized Sentinel 2 Multispectral Satellite Imager (MSI) to generate the study area's Land Use and Land Cover (LULC) data. The LULC distribution was categorized into various groups: (1) water, (2) trees, (3) grass, (4) flooded vegetation, (5) crops, (6) scrub or shrub, (7) built area, (8) bare ground and (9) clouds (see Figure 2). This helped aid the classification of rice paddies, given that the datasets were derived from data catalogue project of ESRI LULC 2021 data **(**Karra et al., 2021). As observed that majority of the study area are surrounded of main croplands.

This contribution has been peer-reviewed. The double-blind peer-review was conducted on the basis of the full paper.
https://doi.org/10.5194/isprs-annals-X-5-2024-41-2024 | © Author(s) 2024. CC BY 4.0 License.

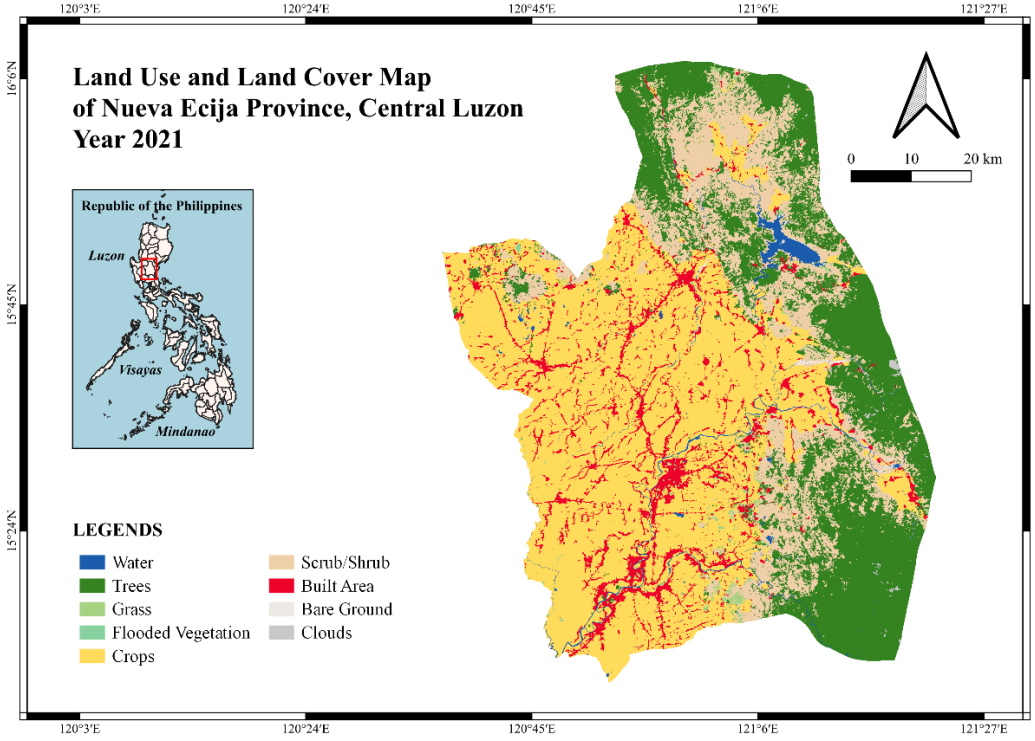

Figure 2. Land Cover Map.

2.4 Image Classification and Accuracy Assessment

The researchers conducted supervised classification of the images through Sentinel 1’s Interferometric Wide Swatch (IW) mode and Vertical/Horizontal (VH) polarization in the Ground Range Detected (GRD) raw images products from the COPERNICUS/S1_GRD collections**.** To create individual VH color composites, researchers set 15-day intervals for the images, while for generating logic color composite bands, multi-temporal images were used. Upon generating band combinations, the color magenta was represented sensitive to rice paddies. In addition, the image classification was based on the color characteristics and signatures (Saadat et al., 2019; Verma et al., 2019).

1st Date (Red) Value	2nd Date (Green) Value	3rd Date (Blue) Value	FCC
Low (~80)	Medium (~140)	High (~180)	
High (~180)	Low (~80)	Medium (~120)	
High (~200)	High (~180)	Low (~70)	

Figure 3. Date composite logic of colors.

Fig. 3 shows the image logic of temporal composite stands as our image combination to classify the rice paddy in the study area (Bourgeau et al., 2009). The blue color range is quite sensitive in other types of crops in the study area which is classified as non-rice. The classified non-rice areas were removed, and the classified areas only remained in the map results. We used the model that showed good accuracy in training and validation with low overprediction results. Temporal changes in the indices clarify the overall well-being of the rice paddies, therefore, the researchers utilized the combined Sentinel 1 and Sentinel 2 images. The specific data from Sentinel 2 goes as follows: Normalized Difference Vegetation Index, Normalized Difference Moisture Index, and Normalized Difference Water Index.

No.	Class	Band Combination	Color
1	Rice	VH2, VH3, VH9	Blue
2	Rice	VH3, VH4, VH9	Magenta
3	Rice	VH3, VH4, VH9	Magenta
4	Rice	VH4, VH5, VH9	Magenta
5	Rice	VH5, VH6, VH9	Magenta
6	Urban	VH2, VH4, VH9	White
7	Water	VH2, VH4, VH9	Black
8	Others	VH6, VH7, VH9	Gray

Table 3. Band color composite combinations.

The appearance of the rice paddies was based on the changes of color in temporal images. By setting each image in every 15 days as an individual band image, we were able to create a temporal color composite. In the early stages of rice crop growth, the sensitivity to color was in the range of blue, and after 30 days, rice began to exhibit sensitivity to colors resembling magenta. Other colors were classified as water, urban, and vegetation (see Table 3). The accuracy assessment is conducted to verify the reliability of the spatial information from the satellite images for the image classification (Lin et al., 2015). In this assessment,

This contribution has been peer-reviewed. The double-blind peer-review was conducted on the basis of the full paper.
https://doi.org/10.5194/isprs-annals-X-5-2024-41-2024 | © Author(s) 2024. CC BY 4.0 License.

ground control points are essential to ensure the trustworthiness and precision of the spatial data. This accuracy assessment was conducted through producer's accuracy, user's accuracy, overall accuracy, proportion, and kappa coefficient (Naikoo et al., 2020).

$$AP = \frac{P_{ii}}{P_{+i}} \quad (1)$$

$$Au = \frac{P_{ii}}{P_{i+}} \quad (2)$$

$$GA = 100\ \frac{\sum_{i=1}^{m} P_{ii}}{n} \quad (3)$$

$$P_L = \left(\frac{A_L}{A_r}\right) \times 100 \quad (4)$$

$$K = \frac{\sum_{ii=1}^{m} P_{ii} - \sum_{i=1}^{c} P_i + P + i}{n^2 - \sum_{i=1}^{m} P_i + P + i} \quad (5)$$

2.5 Vegetation Indices

Normalize Difference Vegetation Index (NDVI) of the reflectance image was also generated. The NDVI was generated for use in the estimation of thermal emissivity of the rice paddy classification. This was carried out using Equation 6 (Campbell and Wynne, 2011).

$$NDVI = NIR - Red / NIR + Red \quad (6)$$

Normalize Difference Moisture Index and Normalize Difference Water Index of the reflectance image collection are calculated using the Equation 7 and 8 (Strashok et al., 2022).

$$NDMI = (NIR – SWIR) / (NIR + SWIR) \quad (7)$$

$$NDWI = (Green – NIR) / (Green + NIR) \quad (8)$$

No.	Date	No.	Date
1	26 June 2021	6	04 September 2021
2	01 July 2021	7	24 September 2021
3	06 July 2021	8	14 October 2021
4	05 August 2021	9	24 October 2021
5	10 August 2021		

Table 4. Sentinel-2 date acquisition.

The NDVI, NDMI and values were obtained for the rice paddy class. The observed mean NDVI, NDMI and NDWI values for the chosen study area are shown in Figure 8. The sentinel – 2 images used are the data collection in Engine Data Catalog Harmonized Sentinel-2 MSI: MultiSpectral Instrument, Level-2A as presented in Table 4. We create a flow chart that outlines the scientific procedure for creating the rice paddy and assessing the rice crop health in classified rice paddies within our study area (see Figure 4). It begins with satellite data acquisition, followed by preprocessing steps to enhance data quality. The next phase involves classifying rice paddies.

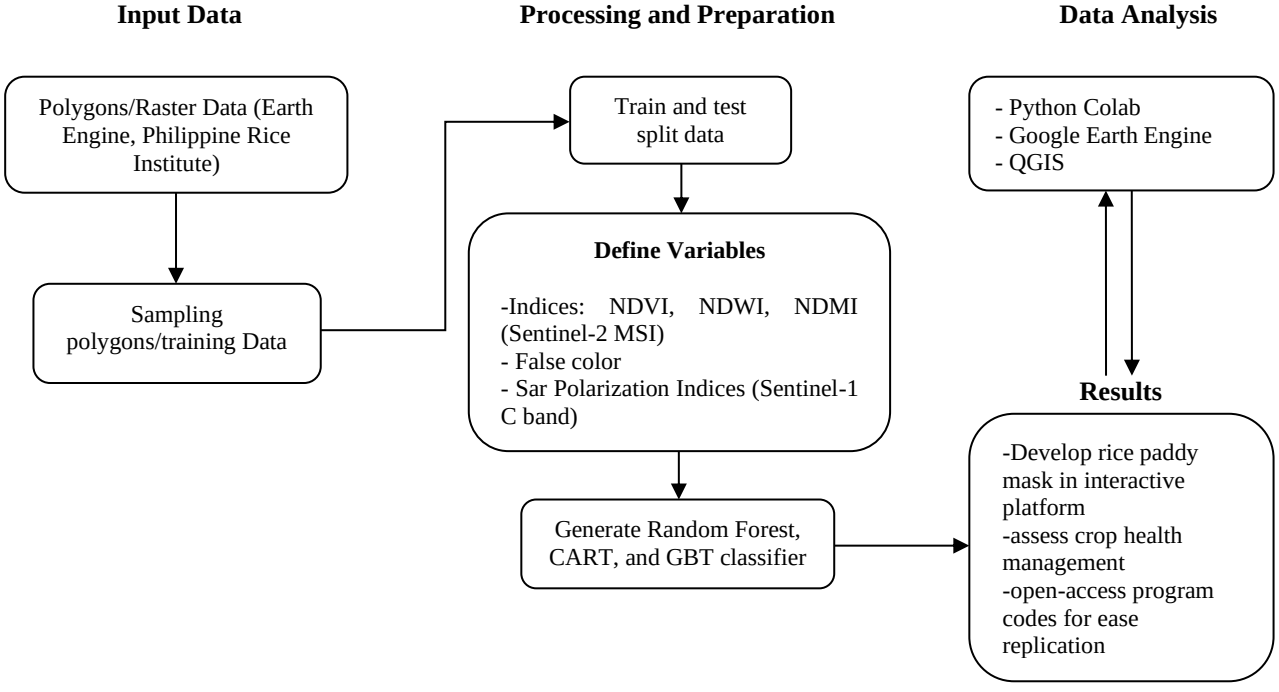

Figure 4. Methodology flow of the project.

3. Results and Discussion

Both microwave data and optical remote sensing images have advantages. Integrating both approaches into the study is essential for increasing the accuracy of the data. The accuracy of the results is higher than that of a single data source when using the integration methods, which are primarily as well (Zhu et al., 2021a). The obtained results showed that all three models achieved high overall accuracy and kappa statistics for rice paddy and non-rice paddy classification. However, the high accuracy of the CART model may indicate overprediction. The classification accuracy met the criterion of at least 80% for the sensor data, with overall rice paddy accuracy ranging from 97% to 99% (Tilahun et al., 2015a). However, the surprisingly high percentage suggests it may be useful to explore further. Further investigation may also be needed to assess the Kappa coefficient values, this will indicate the criterion for good to very good agreement in which the results of the models ranged from 0.96 to 0.99 (see Table 5). These findings demonstrate the high capacity of the decision tree classifier approach in integrating with different

This contribution has been peer-reviewed. The double-blind peer-review was conducted on the basis of the full paper.
https://doi.org/10.5194/isprs-annals-X-5-2024-41-2024 | © Author(s) 2024. CC BY 4.0 License.

remote sensing-derived indices to produce multi-temporal land use/land cover (LULC) maps (Tilahun et al., 2015b).

Class	Machine Learning Model					
	RF		CART		GBT	
	PA	UA	PA	UA	PA	UA
	%					
Rice Paddy	95	99.4	99	99.8	73.8	88.8
Non-Rice Paddy	66	66	87.7	99.3	66.2	84
Accuracy	97		99		98	
Kappa Coefficient	96.2		99		96	

Table 5. Accuracy Assessment of the three model.

Uncertainties and limitation are due to the infrequent use of optical image data in the growing season, which results in features that contribute less to rice identification. This is more prominent during the growing season, as the Philippines is a tropical country that experiences extreme clouds most of the time. Relying primarily on optical data for classification without cloud-polluted time windows can result in lower classification accuracy to a certain extent. On the other hand, microwave data is not restricted by missing images caused by cloud effects (Jiang et al., 2023a). Therefore, SAR data can be applied to reinforce optical data in enhancing the temporal frequency of high-quality observations. Optical and SAR images, when combined, can capture different aspects of rice phenological characteristics. Consolidating images from multiple sensors strengthens both, and moderates the constraints of using a single source. This increases the results of the computational accuracy of the algorithm to an extent (Zhu et al., 2021b; Jiang, et al., 2023b). Integrating images from different bands leverages the strengths of both data sources and mitigates the limitations of a single data source, meanwhile increases the computational results’ accuracy of the algorithm to some extent (Zhu et al., 2021c; Jiang et al., 2023c). By employing three different band combination s for rice identification, we found that combining Sentinel-1 and Sentinel-2 images yields greater accuracy than using either image alone.

3.1 The Spatial Distribution Maps of the Three Models

The results of the supervised classification represented the rice paddies in green pixels, as gathered from Sentinel 1. On the other hand, the CART method identifies more rice paddies which leads to significantly higher user’s and overall accuracy. However, it can be possible due to overprediction. This is being closely resembled by the Random Forest Classification method, where it shows that there are more rice paddies in the eastern region compared to the northern and western regions (see Figure 5.) Furthermore, the results show that temporal signatures reveal changes in band signatures overtime. This indicates that rice planting changes in the area, possibly explaining the downward trend and suggests continuous water flooding.

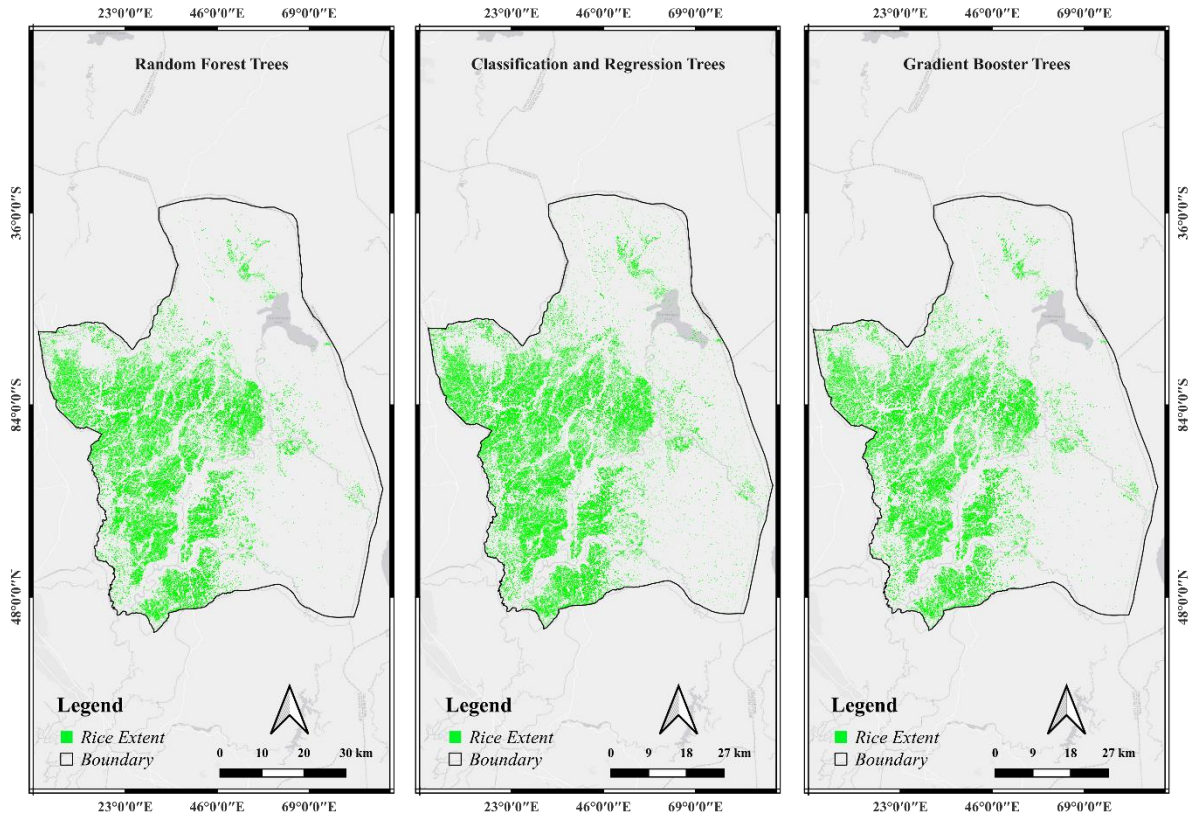

Figure 5. Rice paddy distribution in Nueva Ecija classified by the models from left image (random forest model); middle image (classification regression model) and right image (gradient booster model).

The intensity of backscattering shows the distinct patterns in rice growth phases; specifically noting that high intensity shows the early growing season as it corresponds to water-covered surfaces of young rice paddies. Therefore, as the rice matures, the intensity gradually decreases. It only increases again during the ripening and harvesting periods due to the coinciding situations with satellite imagery observations. It fully decreases after harvesting, as the rice paddies become bare. Results showed that

the NDWI distribution in Guimba is an indication for having well-balanced water availability as reflected from the stable time-series data without excessive flooding. In addition, the NDMI is high over the planting season, specifically in south-eastern areas.

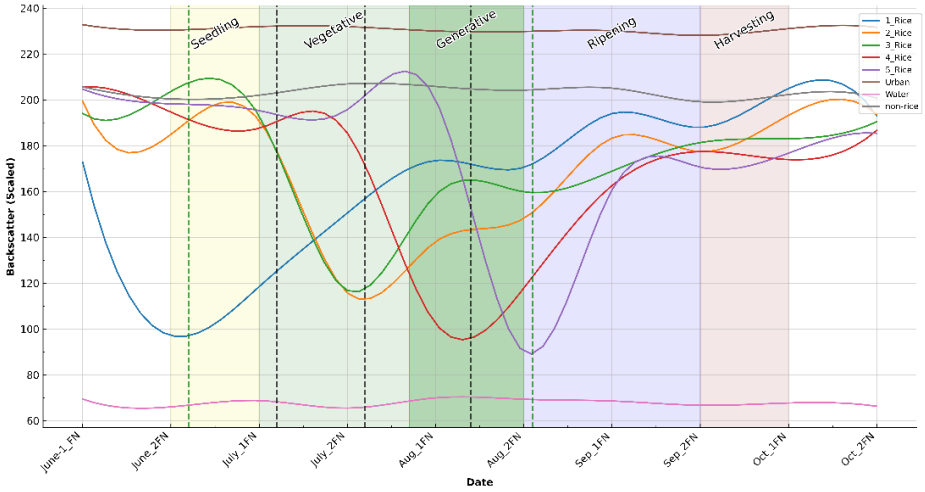

Figure 6. Backscatter signature.

The average soil moisture index is also consistently high, indicating good moisture content, likely caused by the wet season. The NDVI showed gradual increase from June to October (with October having the peak vegetation), suggesting healthy vegetation growth and photosynthetic activity (see Figure 7). The backscatter signature profile of the graph also reveals distinct patterns that align with the rice phenology stages as followed by farmers (Gutierrez et al., 2019a).

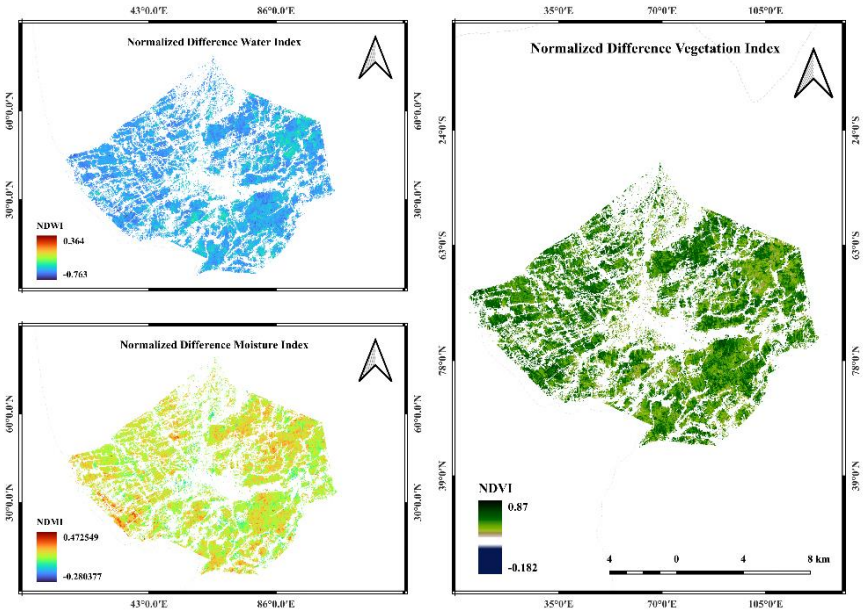

Figure 7. Rice paddy indices distribution in Guimba: upper left (NDWI); bottom left (NDMI) and in the right plot (NDVI).

The high backscatter intensity observed during the early growing season (June 1-15) corresponds to the smooth, water-covered surface of young rice paddies. As the rice plants mature, the backscatter intensity gradually decreases (June 16-30 to July 1-15) due to the increasing roughness of the canopy. This decreasing trend continues until the plants reach full maturity (July 16-31), when the backscatter intensity stabilizes. During the ripening and harvesting phases (August 1-15 to September 1-15), the backscatter intensity increases again as the rice plants dry and the stubble becomes more reflective. The rice planting window in Nueva Ecija, Philippines, is based on the study by (Gutierrez et al., 2019b). The temporal signatures of the radar data match the typical planting season of the area, as most farmers plant during this period when rainfall is most prevalent, providing the essential water source for rice plants. We hypothesized that the sudden drop of the signatures is due to adaptation of farmers in Nueva Ecija in continuous flooding, while as observed that some part of the study area adapts alternating wetting and drying method (Sibayan, 2018). Results in classification of rice paddy areas shows promising results, with approximately 85% of the rice fields in the study area are accurately mapped. However, some limitations persist, particularly regarding temporal mapping due to variations in rice transplanting schedules across different municipalities in Nueva Ecija. Additionally, many rice farmers still rely on natural rainwater for irrigation, while others use artificial irrigation systems, leading to variations in rice

This contribution has been peer-reviewed. The double-blind peer-review was conducted on the basis of the full paper.
https://doi.org/10.5194/isprs-annals-X-5-2024-41-2024 | © Author(s) 2024. CC BY 4.0 License.

planting windows. Our study found that Random Forest (RF) classification yielded reliable results, accurately mapping labelled areas, unlike Classification and Regression Trees (CART) and Gradient Boosting Trees (GBT), which exhibited misclassifications and overprediction issues. The ground image validation was conducted using a mobile phone GPS coordinate tracker (My GPS Coordinates). The coordinates of the classified pixel in Guimba were extracted and used as reference coordinates (latitude: 120.803551, longitude: 15.673251) to validate the presence of rice fields in the study area. During the ground validation visit, the researcher took photographs to confirm the rice paddy plantations, as seen in Figure 8. In the middle box of Figure 8, which was taken near the Coop Rice Mill, the rice plants were observed to be in the generative stage. The left bottom image in the same figure showed rice plants in the ripening stage. Farmers confirmed the stages and status of the rice plants during the ground validation visit. The approximate rice extent areas in each municipality boundary are shown in table 6 appendix.

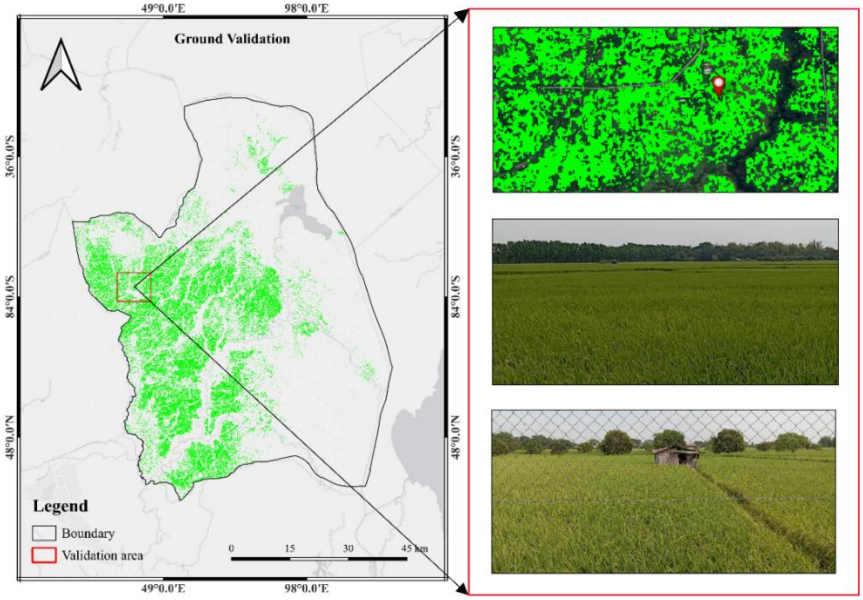

Figure 8. Ground validation in the study area; upper right box (the reference pixel coordinate); middle box (image taken pointing to north) and bottom right box (image taken in east side of the reference coordinates).

4. Conclusion

The present study effectively utilized the Sentinel-1 images for the supervised rice classification and mapping in Guimba, Nueva Ecija. Upon the evaluation of results, the generated classification and map closely aligns with the actual coverage in the area which can be access on the web application platform that we created for ease visualization and replication of codes for further analysis (https://code.earthengine.google.com/2ce5292112782f0e62a01804b3c1a0a3). While the results appeared to be promising, the researchers recommend improvements in classification accuracy by incorporating more annotated samples and exploring alternative machine learning models. Subsequently, the researchers integrated Sentinel-2 data indices to facilitate the monitoring of rice paddy health and growth throughout the rice cultivation period. Through the study’s approach in utilizing remote sensing data for spatial and temporal monitoring, the results will be able to provide valuable insights for farmers in Guimba to optimize water management and enhance rice production. Furthermore, it will also assist in estimating crop yields from the rice paddies, land use planning, and assessing potential environmental impacts.

5. Acknowledgement

We would like to express our sincerest gratitude to Engr. Camille Embalzado, Frank Kelvin Martinez and Jerome Felicidario that helped us throughout this project. Special thanks to Adamson University’s STAR Lab, for their funding and support which has become the foundation in accomplishing this study. We are grateful for your guidance, inputs, and invaluable assistance.

6. References

Agoot L., 2020. PH logs highest rice production rate at 19.44M metric tons: DA. *Philippine News Agency* (22 November 2023).

Breiman, L., 2001. Random Forests, *Machine Learning*, vol. 45, no. 1, pp. 5–32. doi.org/10.1023/a:1010933404324.

Bourgeau-Chavez, L., Riordan, K., Powell, R. B., Miller, N., Nowels, M., 2009. Improving Wetland Characterization with Multi-Sensor, Multi-Temporal SAR, and Optical/Infrared Data Fusion. In *InTech* eBooks. doi.org/10.5772/8327.

Campbell, J. B., Wynne, R. H., 2011. Introduction to remote sensing. *Guilford press*.

Gislason, P. O., Benediktsson, J. A., Sveinsson, J. R., 2006.Random Forests for land cover classification. *Pattern Recognition Letters*, 27(4), 294–300. doi.org/10.1016/j.patrec.2005.08.011.

Gutaker, R. M., Groen, S. C., Bellis, E. S., Choi, J. Y., Pires, I. S., R. Kyle Bocinsky, Slayton, E. R., Wilkins, O., Castillo, C. C., Sónia, N., Oliveira, M. M., Fuller, D. Q., d’Alpoim Guedes, Lasky, J. R., Purugganan, M. D., 2020. Genomic history and ecology of the geographic spread of rice. *Nature Plants*, 6(5), 492–502. doi.org/10.1038/s41477-020-0659-6.

Gutierrez, M. A., Paguirigan, N. M., Raviz, J., Mabalay, M. R., Alosnos, E., Villano, L., Asilo, S., Arocena Jr., A., Maloom, J., and Laborte, A., 2019. The Rice Planting Window in the

Philippines: An Analysis Using Multi-temporal Sar Imagery. *International Archives of the Photogrammetry, Remote Sensing and Spatial Information Sciences*, vol. XLII-4/W19, pp. 241–248. doi.org/10.5194/isprs-archives-XLII-4-W19-241-2019.

Jiang, Q., Tang, Z., Zhou, L., Hu, G., Deng, G., Xu, M., Sang, G., 2023. Mapping Paddy Rice Planting Area in Dongting Lake Area Combining Time Series Sentinel-1 and Sentinel-2 Images. *Remote Sensing*, 15(11), 2794–2794. doi.org/10.3390/rs15112794.

Joly, A., Wehenkel, L., Geurts, P., 2019. Gradient tree boosting with random output projections for multi-label classification and multi-output regression. *arXiv*. doi.org/10.48550/arXiv.1905.07558.

Karra, K., Kontgis, C., Statman-Weil, Z., Mazzariello, J. C., Mathis, M. M., Brumby, S. P., 2021. Global land use / land cover with Sentinel 2 and deep learning. *IEEE Xplore*. doi.org/10.1109/igarss47720.2021.9553499.

Lin, C., Wu, C., Tsogt, K., Ouyang, Y., Chang, C., 2015. Effects of atmospheric correction and pansharpening on LULC classification accuracy using WorldView-2 imagery. Information *Processing in Agriculture*, 2(1), 25–36. doi.org/10.1016/j.inpa.2015.01.003.

Naikoo, M. W., Rihan, M., Ishtiaque, M., Shahfahad., 2020. Analyses of land use land cover (LULC) change and built-up expansion in the suburb of a metropolitan city: Spatio-temporal analysis of Delhi NCR using landsat datasets. *Journal of Urban Management*, 9(3), 347–359. doi.org/10.1016/j.jum.2020.05.004.

Philippines Deforestation Rates and Statistics | GFW, *globalforestwatch.org* (12 December 2023).

Qi, L., Yue, C. R., 2011. Remote sensing image classification based on CART decision tree method. *Forest Inventory and Planning*, 36(2), 62-66.

Raviz, J., Laborte, A., Barbieri, M., Mabalay, M. R., Garcia, C., Bibar, J.E.A., Mabalot, P., Gonzaga, H., 2016. Mapping and monitoring rice areas in Central Luzon, Philippines using X and C-band SAR imagery. In *37th Asian Conference on Remote Sensing*.

Saadat, M., Hasanlou, M., Homayouni, S., 2019. Rice Crops Mapping Using Sentinel -1 Time Series Images Case Study: Mazandaran, Iran. *The International Archives of the Photogrammetry, Remote Sensing and Spatial Information Sciences*, XLII-4/W18, 897–904. doi.org/10.5194/isprs-archives-xlii-4-w18-897-2019.

Shi, Y., Li, J., Li, Z., 2018. Gradient boosting with Piece-Wise Linear Regression trees. a*rXiv*, Cornell University. doi.org/10.48550/arxiv.1802.05640.

Sibayan, E. B., Samoy-Pascual, K., Grospe, F. S., Casil, M. E. D., Tokida, T., Padre, A. T., Minamikawa, K., 2018. Effects of alternate wetting and drying technique on greenhouse gas emissions from irrigated rice paddy in Central Luzon, Philippines. *Soil science and plant nutrition*, 64(1), 39-46. doi.org/10.1080/00380768.2017.1401906.

Silva, J. V., Reidsma, P., Laborte, A. G, Martin, K. I., 2017. Explaining rice yields and yield gaps in Central Luzon, Philippines: An application of stochastic frontier analysis and crop modelling. *European Journal of Agronomy*, 82, 223–241. doi.org/10.1016/j.eja.2016.06.017.

Strashok, O., Ziemiańska, M., Strashok, V., 2022. Evaluation and correlation of normalized vegetation index and moisture index in Kyiv (2017–2021). *Journal of Ecological Engineering*, 23(9), 212–218. doi.org/10.12911/22998993/151884.

Tilahun, A., Teferie, B., 2015. Accuracy Assessment of Land Use Land Cover Classification using Google Earth. *American Journal of Environmental Protection*, vol. 4, no. 4, p. 193. doi.org/10.11648/j.ajep.20150404.14.

Verma, A., Kumar, A., Lal, K., 2019. Kharif crop characterization using combination of SAR and MSI Optical Sentinel Satellite datasets. *Journal of Earth System Science*, vol. 128, no. 8. doi.org/10.1007/s12040-019-1260-0.

Voisin, A., Krylov, V. A., Moser, G., Zerubia, J., 2014. Supervised Classification of Multisensory and Multiresolution Remote Sensing Images with a Hierarchical Copula-Based Approach. *IEEE Transactions on Geoscience and Remote Sensing*, 52(6), 3346–3358. doi.org/10.1109/tgrs.2013.2272581.

Ustuner, M., Sanli, F. B., Abdikan, S., Bilgin, G., Goksel, C., 2019. A Booster Analysis of Extreme Gradient Boosting for Crop Classification using PolSAR Imagery. *IEEE Xplore*. doi.org/10.1109/agro-geoinformatics.2019.8820698.

Zhu, L., Liu, X., Wu, L., Liu, M., Lin, Y., Meng, Y., Ye, L., Zhang, Q., Li, Y., 2021. Detection of paddy rice cropping systems in southern China with time series Landsat images and phenology-based algorithms. *Geoscience & Remote Sensing*, 58(5), 733-755. doi.org/10.1080/15481603.2021.1943214.

7. Appendix

Municipality	Area (km^2)	Municipality	Area (km^2)	Municipality	Area (km^2)	Municipality	Area (km^2)
Guimba	9.656	Licab	1.916	Gapan City	4.598	Gabaldon	0.363
Munoz	4.022	Santo Domingo	3.153	Jaen	4.817	Bongabon	0.535
Talugtug	2.391	Aliaga	4.480	San Leonardo	1.432	General Mamerto	2.769
Cuyapo	3.349	Zaragoza	2.716	Penaranda	0.976	Llanera	2.893
Nampicuan	2.149	Talavera	3.322	Santa Rosa	4.064	Rizal	4.115
San Jose City	2.361	San Antonio	4.421	General Tinio	0.897	Pantabangan	0.280
Lupao	0.963	San Isidro	2.113	Cabanatuan	3.881	Quezon	2.729
Carranglan	1.656	Cabiao	2.549	Palayan City	0.196	Laur	0.947

Table 6. Estimated rice paddy area per municipal boundary.